Geomechanics and Engineering, *Vol. 23, No. 5 (2020) 455-466*
DOI: https://doi.org/10.12989/gae.2020.23.5.455

Numerical simulation of the influence of interaction between Qanat and tunnel on the ground settlement

Vahab Sarfarazi*[1] and Abdollah Tabaroei[2a]

[1]*Department of Mining Engineering, Hamedan University of Technology, Hamedan, Iran*
[2]*Department of Civil Engineering, Eshragh Institute of Higher Education, Bojnourd, Iran*

(Received August 6, 2020, Revised November 11, 2020, Accepted November 26, 2020)

Abstract. This paper presents analysis of the interaction between tunnel and Qanat with a particular interest for the optimization of Qanat shape using the discrete element code, PFC2D, and the results will be compared with the FEM results of PLAXIS2D. For these concerns, using software PFC2D based on Discrete Element Method (DEM), a model with dimension of 100m * 100 m was prepared. A circular tunnel with dimension of 9 m was situated 20 m below the ground surface. Also one Qanat was situated perpendicularly above the tunnel roof. Distance between Qanat center and ground surface was 8 m. Five different shapes for Qanat were selected i.e., square, semi-circular, vertical ellipse, circular and horizontal ellipse. Confining pressure of 5 MPa was applied to the model. The vertical displacement of balls situated in ground surface was picked up to measure the ground subsidence. Also two measuring circles were situated at the tunnel roof and at the Qanat roof to check the vertical displacements. The properties of the alluvial soil of Tehran city are: γ_{dry}=19 (KN/m^3), E= 750 (kg/cm^2), ν=0.35, c=0.3 (kg/cm^2), φ=34°. In order to validate the DEM results, a comparison between the numerical results (obtained in this study) and analytical and field monitoring have been done. The PFC2D results are compared with the FEM results. The results shows that when Qanat has rectangular shape, the tensile stress concentration at the Qanat corners has maximum value while it has minimum value for vertical ellipse shape. The ground subsidence for Qanat rectangular shape has maximum value while it has minimum value for ellipse shape of Qanat. The vertical displacements at the tunnel roof for Qanat rectangular shape has maximum value while it has minimum value for ellipse shape of Qanat. Historical shape of Qante approved the finding of this research.

Keywords: tunnel; Qanat shape; PFC2D; PLAXIS2D

1. Introduction

The demand for construction of subways, underground passages, and urban pipe corridors is increasing due to limitation of space for surface transport in the urban areas (Liao 2008, Shen 2011, Zhang 2016). There are many existing underground structures, such as Qanats, pile foundations, municipal pipelines and tunnels, which may hinder the development of three-dimensional underground space use. Therefore, new tunnel construction often needs to bypass existing structures with a parallel or cross configuration (Do 2014, Liu *et al.* 2011, Zhang 2020). In addition, the construction of new underground structures affects the normal operation of ground surface structures. Thus, complex crossing tunnels have potential construction risks and safety hazards and adversely affect adjacent structures (Zhang and Huang 2014). Gould *et al.* (2009) analyzed data from 39 687failures documented by Australian water authorities over a 10 year period. Field crews responsible for pipeline repairs verified that a significant number of these incidents were a result of ground movement. Chan *et al.* (2007) identified a "clear relationship" between City West Water Ltd. (Melbourne, Australia) pipeline network failure rates and seasonal variation of soil moisture content. Pratt *et al.* (2011) analysed a database of 8100 failures in cast iron and reinforced concrete water pipelines that occurred over a 10 year period in Western Australia, and reached similar conclusions. In Tehran province in Iran, the subway tunnels is adjacent to Qanats. Therefore, it is necessary to fully understand the land subsidence caused by the construction of tunnel and the impact on existing adjacent Qanat. At present, there are mainly three methods for studying the tunnels: (1) empirical or field measurement methods, (2) the model test method, and (3) the numerical analysis method. Based on the field survey data, empirical methods as implemented in a previous study were used to calculate the change of the internal force of the tunnel lining caused by surface settlement and adjacent construction (Harris 1994, Tan 2011, Zhang *et al.* 2013, Zhang *et al.* 2019). It is clear that field observations remain the key to understanding the interaction between adjacent tunnels. Unfortunately, field data are often incomplete. The structural forces induced in tunnel linings are thus hard to obtain. The empirical and analysis method, using the superposition method (Yang 2011), is based on the prediction of each tunnel's individual excavation, and the

*Corresponding author, Associate Professor
E-mail: sarfarazi@hut.ac.ir
[a]Assistant Professor
E-mail: a.tabaroei@eshragh.ac.ir

ISSN: 2005-307X (Print), 2092-6219 (Online)

final settlement curve is obtained by superposition. In general, the superposition method cannot rigorously consider the effect of an existing tunnel or the repeated unloading of the ground caused by the previous excavation of the first tunnel; therefore, the settlement curves do not predict the final displacement very well (Divall and Goodey 2015). Model tests, in particular the centrifuge model test, are another preferred choice for the study of underground works since the same stress state in the tests is used to simulate the actual stress state of the soil (Li 2014, Ng 2013). However, the model test study is difficult to implement for large-scale tests. Furthermore, the cost of the model test is high, which limits its application. Numerical analysis, as a convenient and effective research tool, has been widely used by researchers and engineers (Jiang 2012, 2014, Jin 2019, Katebi 2015, Moller, 2006, Zhang *et al.* 2016, Zhang 2018, Zhang 2020). As far as multi-tunnel excavation is concerned, the introduction of appropriate boundary conditions and appropriate constitutive models (Zhang 2020, Zhang 2019, Zhang 2018, Greenwood 2001, Wang 2003, Hage Chehade 2008, Do *et al.* 2014, Hu 2020, Lin 2020a, b, Sarfarazi 2014, Sarfarazi 2016a-c, Haeri 2016a-d) makes it possible to predict land subsidence using numerical analysis methods.

This paper presents analysis of the interaction between tunnel and Qanat with a particular interest for the optimization of adequate shape using the discrete element code, PFC2D, and the results will be compared with the FEM results of PLAXIS2D. In order to validate the DEM results, a comparison between the numerical results (obtained in this study) and analytical and field monitoring have been done. The Discrete Element Method is selected for modeling of discontinuous nature of coarse-grain alluvial soils. Parametric study analyses were conducted for five adequate shape to investigate their influence on the soil settlement resulting from the tunnel construction.

2. Discrete element method

The DEM was introduced by Cundall (1971) for the analysis of rock-mechanics problems, and then applied to soils by Cundall and Strack (1979). PFC2D is classified as a discrete element code since it allows finite displacements and rotations of discrete bodies, including complete detachment, and recognizes new contacts automatically as the calculation progresses. The code can be viewed as a simplified implementation of the DEM because of the restriction to rigid circular particles, Itasca Consulting Group 2004. The calculations performed in the DEM alternate between the application of Newton's second law to the particles and a force-displacement law at the contacts. Newton's second law is used to determine the motion of each particle arising from the contact and body forces acting upon it, while the force-displacement law is used to update the contact forces arising from the relative motion at each contact Cundall and Strack(1979). The presence of walls in the code requires only that the force-displacement law accounts for ball-wall contacts. Newton's second law is not applied to walls, since the wall motion is specified by the user Itasca Consulting Group 2004. When two particles

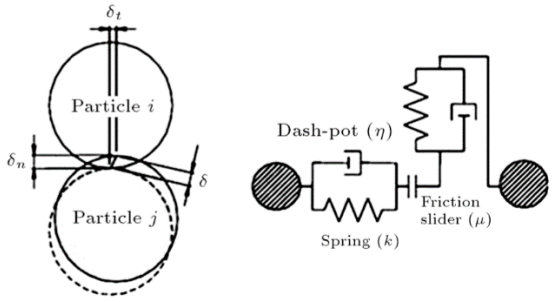

Fig. 1 Contact force model, Itasca Consulting Group (2004)

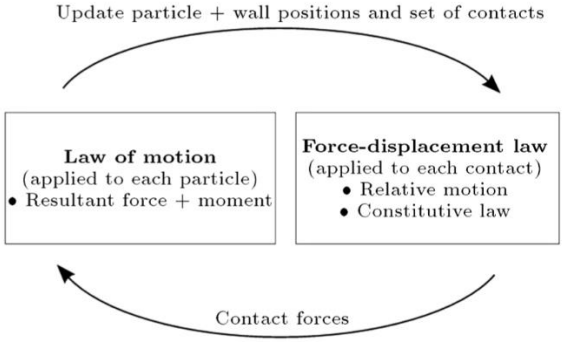

Fig. 2 Calculation cycle in PFC2D, Cundall and Strack (1979)

collide, they actually deform. The overlap displacement is assumed as deformation in the DEM as shown in Fig. 1(a). Then, the DEM contact is composed of a spring, a dash-pot, and a friction slider as shown in Fig. 1(b), Kanou 2003. The calculation cycle in the code is an explicit time stepping algorithm that consists of the repeated application of the law of motion to each particle, a force-displacement law to each contact, and a constant updating of wall positions. Contacts, which may exist between two balls or between a ball and a wall, are formed and broken automatically during the course of a simulation. The calculation cycle is illustrated in Fig. 2, Itasca Consulting Group 2004. The limitations of DEM is (Donze *et al.* 2009): (a) Fracture is closely related to the size of elements, and that is so-called size effect. (b) Cross effect exists because of the difference between the size and shape of elements with real grains. (c) In order to establish the relationship between the local and macroscopic constitutive laws, data obtained from classical geomechanical tests which may be impractical are used.

3. Numerical modeling

PFC2D is a distinct element computer program designed to simulate the mechanical behavior of bonded or unbounded granular materials. The soil material is modeled as a collection of circular particles that can interact through normal and shear springs. Under the applied load, the bonds between particles can break and a small crack can form, Itasca Consulting Group (2004). Although the code can simulate a particulate media, any circular element in this program does not necessarily model a particle in the real material as the two-dimensional nature of the program

limits particles to disks or cylinders. Hence, the code can be considered as an attempt to mimic the basic mechanical features of the actual material. Therefore, it is not possible to use the geotechnical parameters directly in PFC2D, and it is necessary to obtain the numerical modeling parameters using calibration of real triaxial tests.

3.1 Particle generation

The particle radii were chosen to have a relatively uniform distribution in the sample. Particle in the code does not need to correspond to areal grain in the actual material, Fakhimi *et al.* (2002). In PFC2D, particles are created at their final radii in sufficient numbers to achieve the desired porosity for the production of the real in-situ stresses. In this paper, the minimum radius of the particle assembly is R_{min} = 5 cm and R_{max}=R_{min} = 3, Fakhimi *et al.* (2002). They are placed at random positions in the given area, which leads to some large overlaps and correspondingly large forces. Then, the resulting large initial velocities may be sufficient to allow some particles to escape through the confining walls. To prevent this, the kinetic energy is reduced to zero several times during the first few cycles; then, convergence to equilibrium proceeds normally, Itasca Consulting Group (2004).

3.2 Boundary and initial conditions

The soil layer is underlined at the depth of H = 100 m. The lateral extension of the soil mass is equal to 100 m. The extension ensures the absence of boundary effect on the numerical modeling of the tunnel construction. The number of particles in the domain is approximately 85000. Normally, a particle assembly is created and compacted within a set of confining walls. These walls can continue to act as boundary constraints. The initial conditions in a granular assembly are partly inherited from the generation and compaction phases. The concept of stress in a discontinuous medium is different from that in a continuous. There is no meaning to the term "stress at a point", because forces may fluctuate wildly from point to point. An estimate of stress is only possible over a finite volume of space. A numerical servo-mechanism is applied iteratively to arrive at the radius expansion necessary to achieve the required mean stress, Itasca Consulting Group (2004). There are various methods for achieving a desired initial stress state. Parameters such as density, porosity, and stiffness coefficients affect the initial stress, so if it turns out changes in parameters, it bring about changes in stress, Itasca Consulting Group (2004).

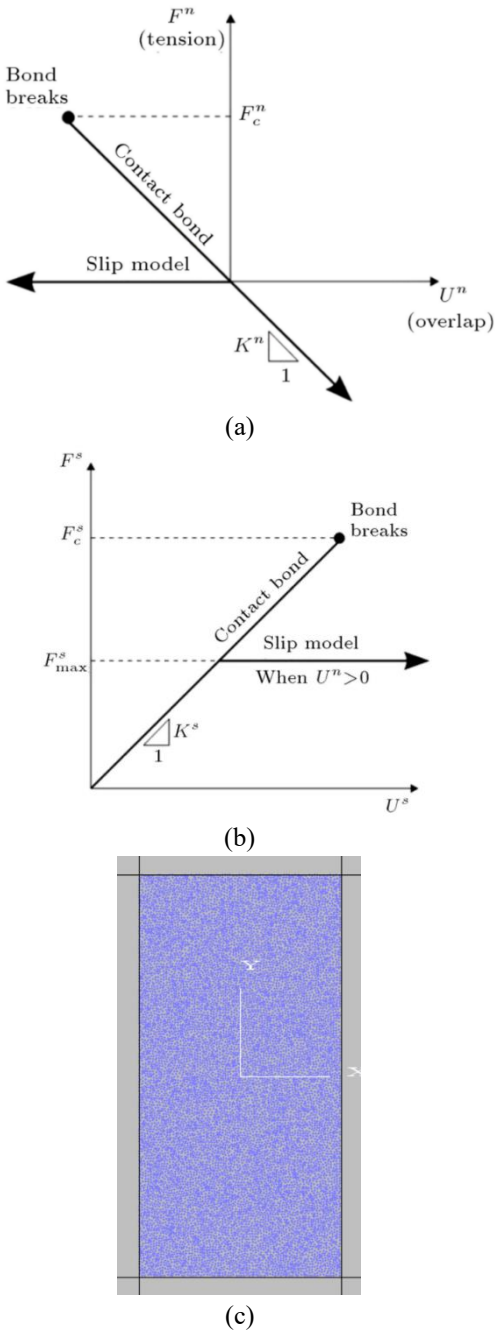

Fig. 3 Constitutive behavior for the contact occurring at a point regarding contact-bond model Itasca Consulting Group (2004), (a) normal component of contact force, (b) shear component of contact force and (c) a biaxial test by confining a rectangular sample

3.3 Determination of proper micro-parameters (calibration)

The overall constitutive behavior of a material is simulated in PFC2D by associating a constitutive model with each contact. The constitutive model acting at a particular contact consists of three parts: A stiffness model, a slip model, and a bonding model. The stiffness model provides an elastic relation between the contact force and relative displacement. The slip model enforces a relation between shear and normal contact forces such that the two contacting balls may slip relative to one another. The bonding model serves to limit the total and shear forces that the contact can carry by enforcing bond-strength limits. The two basic bonding models supported in the code are: A contact-bond model and a parallel-bond model. Both bonds can be envisioned as a kind of glue joining the two particles. The contact-bond glue is of a vanishingly small size that acts only at the contact point, while the parallel-bond glue is of a finite size that acts over either a circular or

Table 1 the properties of the alluvial soil of Tehran city

γ_{dry} (KN/m^3)	E (Kg/cm^2)	ν	C(Kg/cm^2)	φ(°)
19	750	0.35	0.3	34

Table 2 Determined micro-parameters in PFC2D (getting from calibration)

Soil properties	Kn (N/m)	Ks (N/m)	n-bond (N/m)	s-bond (N/m)	friction	porosity	Density (Kg/m^3)
	2e8	1e8	0.42e6	0.35e6	0.1	0.14	2500

Table 3 The properties of the alluvial soil of Porto city

γ_{dry} (KN/m^3)	E (Kg/cm^2)	ν	C(Kg/cm^2)	φ(°)
18.7	700	0.3	0.45	29

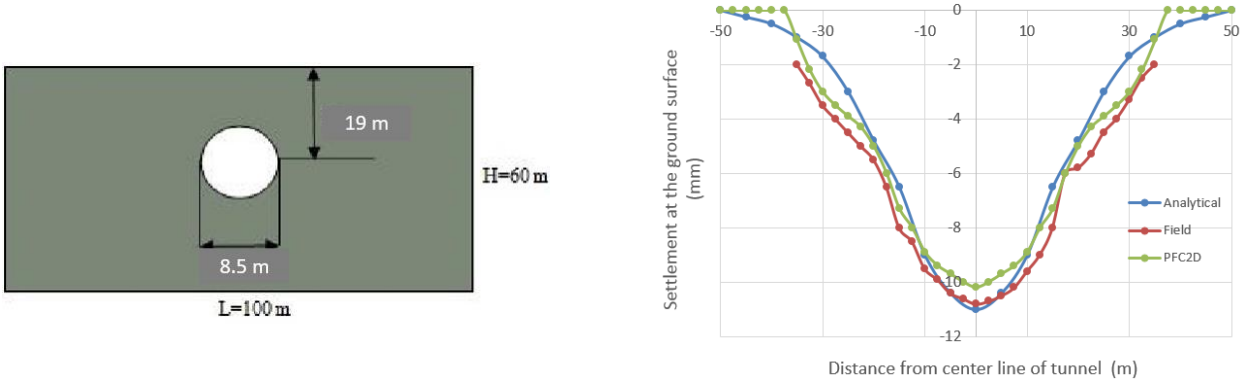

(a) (b)

Fig. 4 (a) The schematic view of single tunnel geometry and (b) The comparison of ground surface settlement profiles obtained from numerical, analytical and field methods

rectangular cross section lying between the particles. The contact-bond can only transmit a force, while the parallel-bond can transmit both a force and a moment. The contact-bond and parallel-bond can be viewed as cohesion for soils and rocks, respectively. Hence, in this research, the contact-bond model is used. Constitutive behavior for contact occurring at a point is shown in Fig. 3 regarding contact-bond model, Itasca Consulting Group (2004). Keeping constant values of stiffness and friction coefficients, PFC2D's input parameters including bond coefficients, vary until the behavior of the numerical sample matches that of the physical sample. In PFC2D, a biaxial test by confining a rectangular sample (comprised of a compacted particle assembly) within four walls is simulated (Fig 3(c)). The top and bottom walls simulate loading platens, and the left and right walls simulate the confinement experienced by the sample sides. The sample is loaded in a strain-controlled mode by specifying the velocities of the top and bottom walls. The stresses and strains experienced by the sample are determined in a macro-mode by summing the forces acting upon, and relative distance between the appropriate walls. Material response is evaluated by tracking the various stress and strain quantities. Axial deviatoric stress versus axial strain for biaxial test on bonded granular material was drawn, and then Mohr's circle was drawn to reach failure envelope of laboratory. Table 1 summarizes the properties of the alluvial soil of Tehran city used in this study, Fakhimi *et al.* (2002). The determined micro-parameters (getting from calibration) are listed in Table 2 based on strength and stiffness criteria.

3.4 Verification

In order to validate the DEM results, a comparison between the numerical results (obtained in this study) and analytical and field monitoring, Geological and Geotechnical Report (2010), is presented in Fig. 4. The field case study has been selected for single tunnel of Porto subway in Portugal to validate the accuracy of calibration method (Guglielmetti 2007). Fig 1 shows the schematic view of single tunnel geometry. Table 3 shows the properties of the alluvial soil of Porto subway. The analytical method is a criteria rendered by Tian (2020). The maximum surface settlement obtained from numerical analysis is 1.1 cm and 1.09 for field monitoring. There is a very good agreement between DEM and field results.

3.5 Tunnel and Qanat modeling

A model with dimension of 100 m * 100 m was prepared. This is due to restriction of tunnel dimension. The boundary of model should be far from the tunnel wall to avoid the boundary effect on the tunnel behavior. A circular tunnel with dimension of 9 m was situated 18 m below the

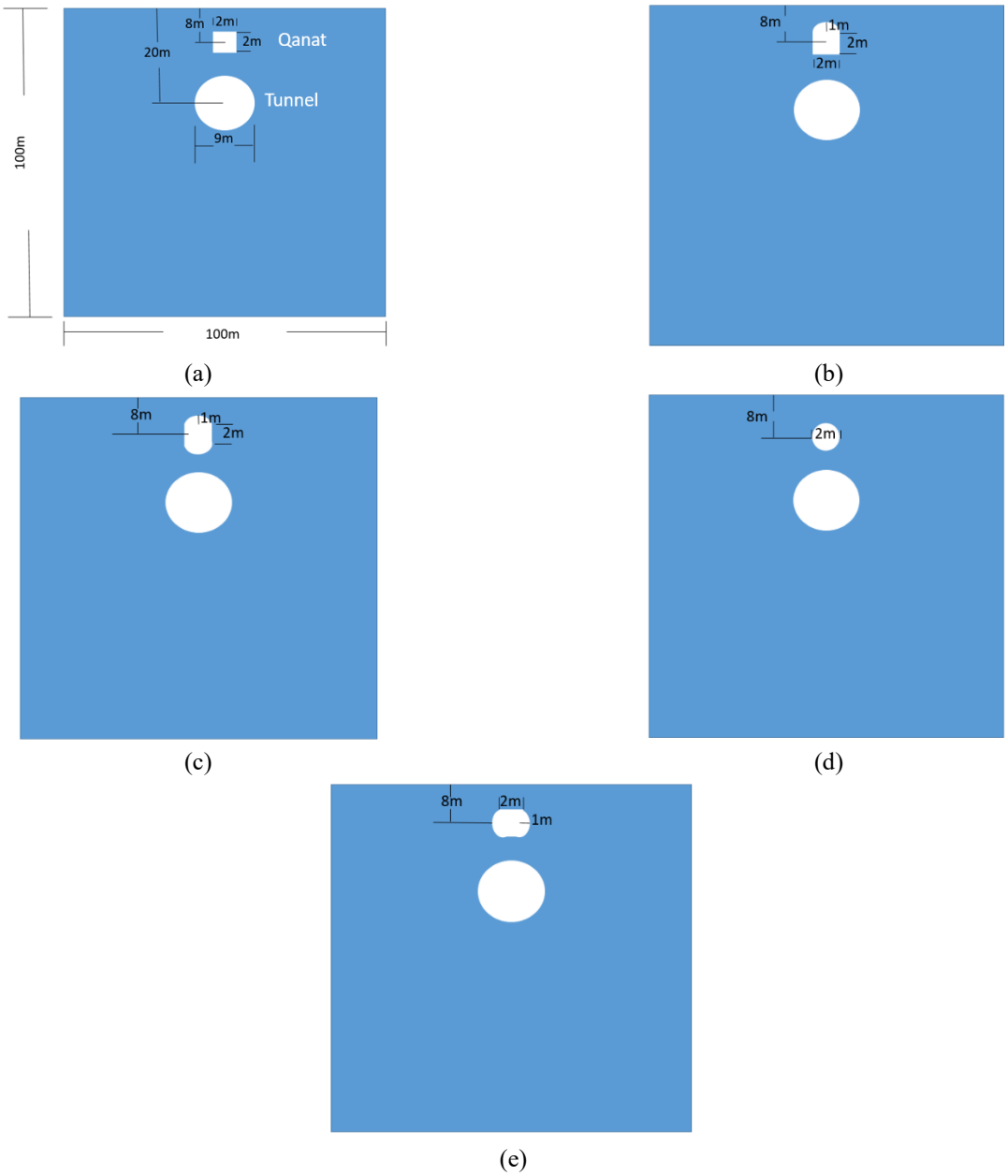

Fig. 5 the schematic view of Qanat and tunnel; Qanat shape was, (a) square, (b) semi-circular, (c) vertical ellipse, (d) circular and (e) horizontal ellipse

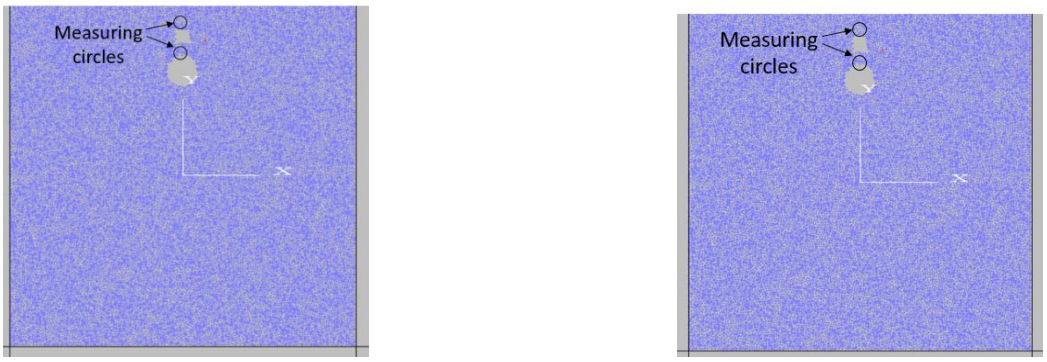

Fig. 6 The circular tunnel in PFC2d; Qanat shape was, (a) square, (b) semi-circular, (c) vertical ellipse, (d) circular and (e) horizontal ellipse

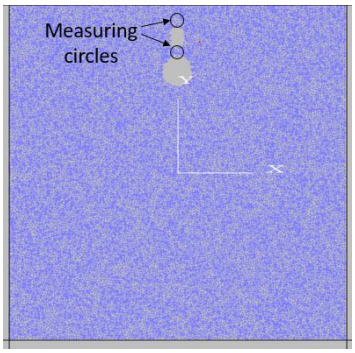

(c)

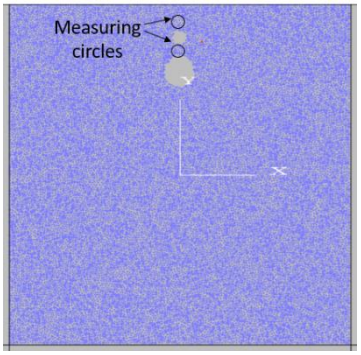

(d)

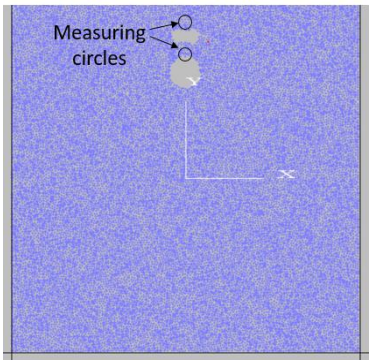

(e)

Fig. 6 Continued

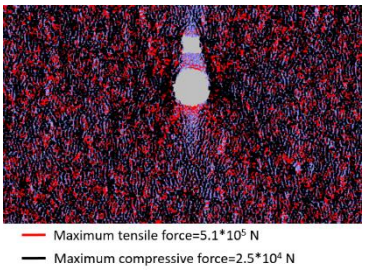

(a)

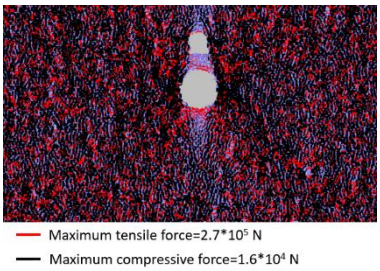

(b)

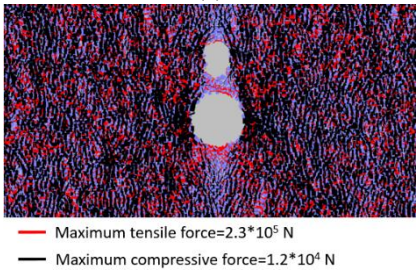

(c)

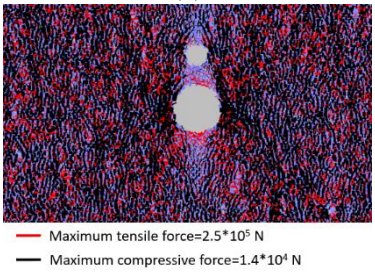

(d)

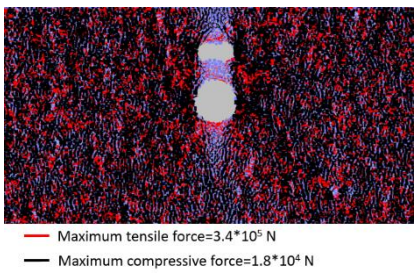

(e)

Fig. 7 Numerical model of Qanat and tunnel, (a) square, (b) semi-circular, (c) vertical ellipse, (d) circular and (e) horizontal ellipse

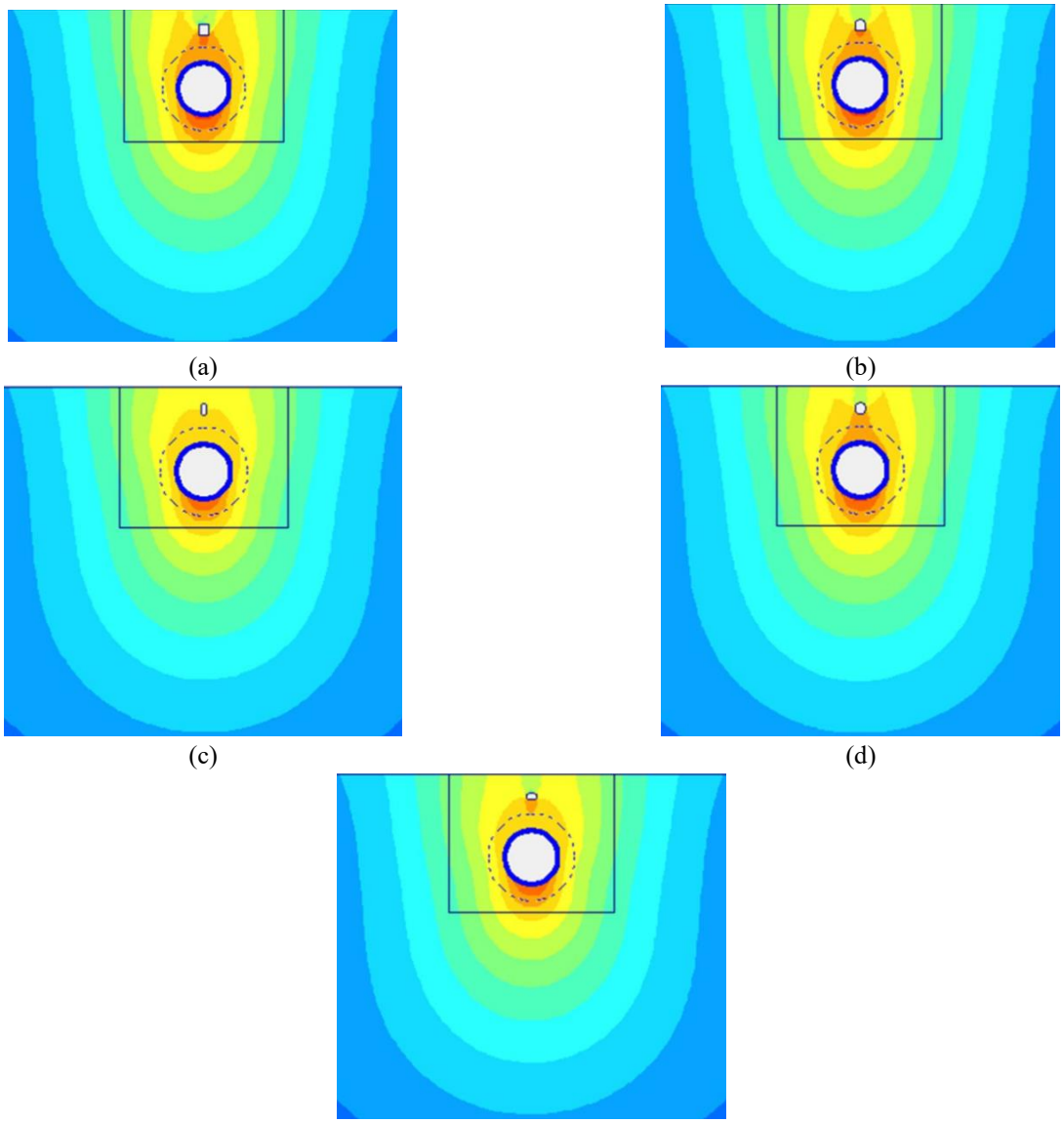

Fig. 8 Vertical displacement contour in PLAXIS model; Qanat shape was, (a) square, (b) semi-circular, (c) vertical ellipse, (d) circular and (e) horizontal ellipse

ground surface. Also one Qanat was situated perpendicularly above the tunnel roof. Distance between Qanat center and ground surface was 8 m. five different shapes for Qanat were selected i.e., square, semi-circular, vertical ellipse, circular and horizontal ellipse. Fig. 5 shows the schematic view of Qanat and tunnel. Also, Fig 6 shows PFC model used for the analysis. Confining pressure of 5 MPa was applied to the model. The vertical displacement of balls situated in ground surface was picked up to measure the ground settlement. Also, two measuring circles were situated at the tunnel roof and at the Qanat roof to check the vertical displacement. Concurrent with PFC2D simulation, Plaxis2d was used for settlement evaluation. Model dimension in Plaxis2d was similar to PFC2D model. The PFC2D results are compared with the FEM results. The water table is considered in the bottom of the model at depth of 50 m, and the influence of surface structures in comparison to tunnel overburden is negligible.

4. Numerical results

4.1 The contact bond forces in PFC2D models

The contact bond force distribution (as shown in Fig. 7 (a)-7(e)) illustrates the state of force vectors within the modelled samples for five shapes of Qanat (i.e., square, semi-circular, vertical ellipse, circular and horizontal ellipse). The red and dark lines shown in Figs. 7 a-e represent the tensile and compression force vectors in the model, respectively. The coarse lines and their accumulation show the areas where larger forces are induced within the model. The value of maximum tensile force and maximum compressive force were registered on these figures. It can be easily seen that the maximum tensile forces are concentrated at top and bottom of the spaces while the maximum compressive forces are concentrated at left and right sides of the spaces. The both of maximum tensile

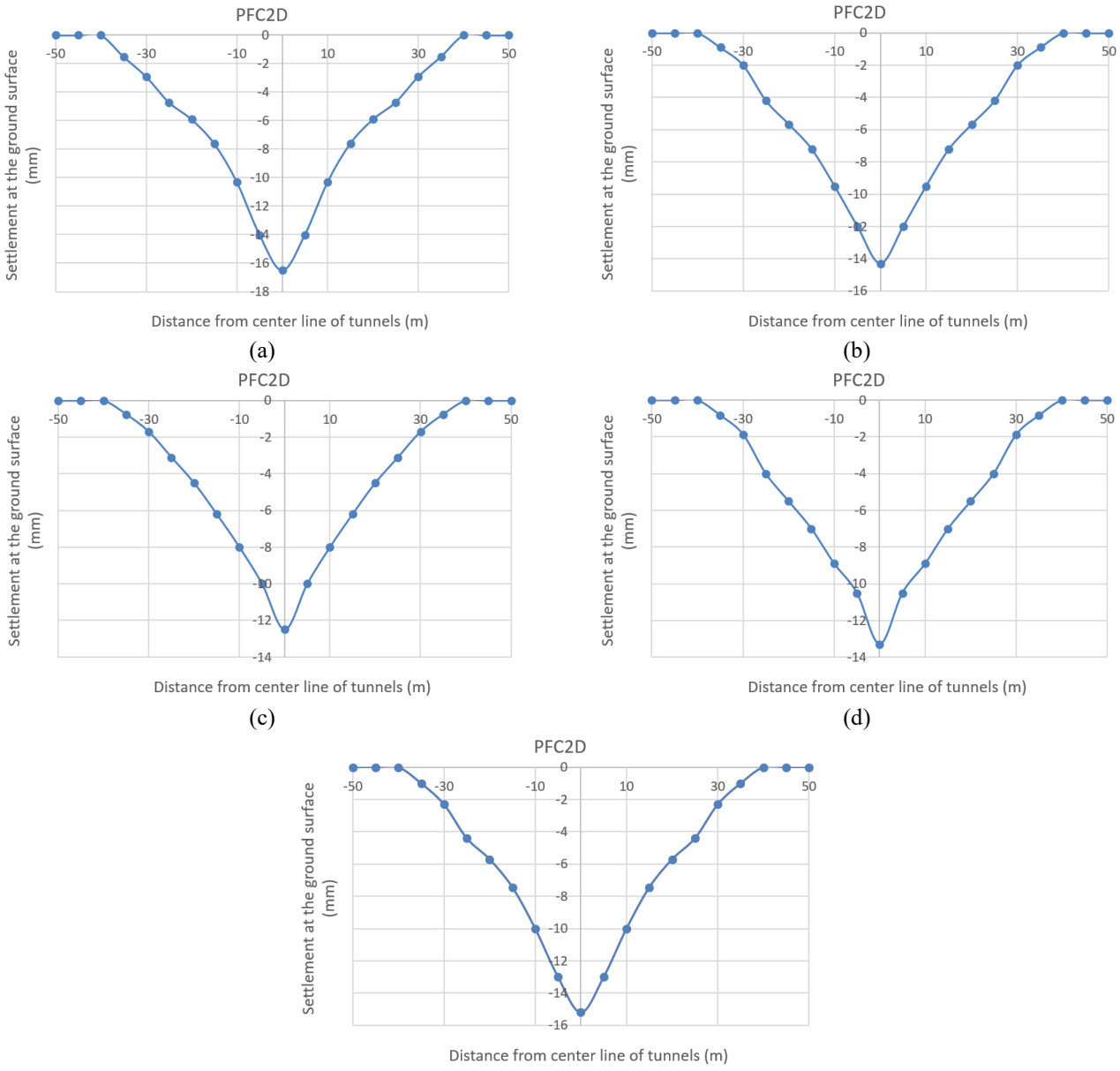

Fig. 9 PFC2D model of Qanat and tunnel, (a) square, (b) semi-circular, (c) vertical ellipse, (d) circular and (e) horizontal ellipse

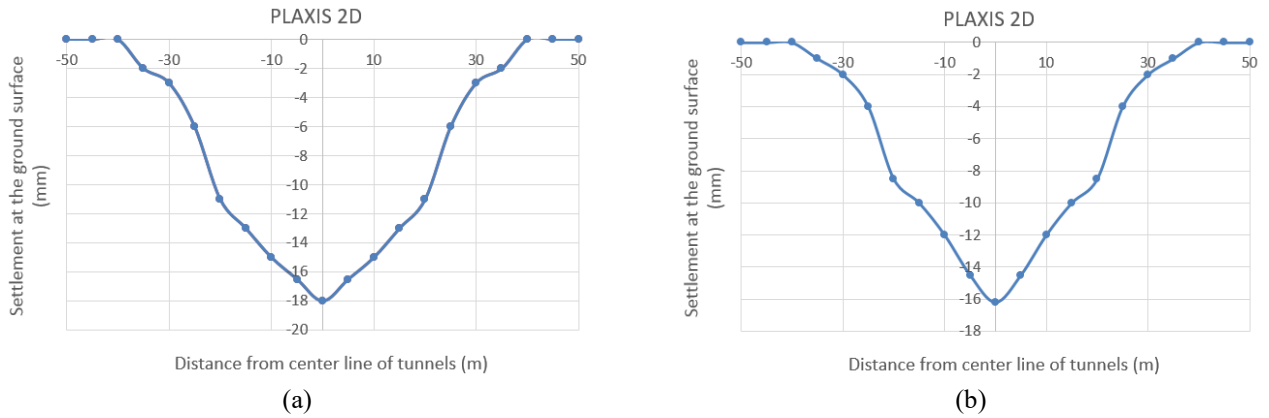

Fig 10 PLAXIS model of Qanat and tunnel, (a) square, (b) semi-circular, (c) vertical ellipse, (d) circular and (e) horizontal ellipse

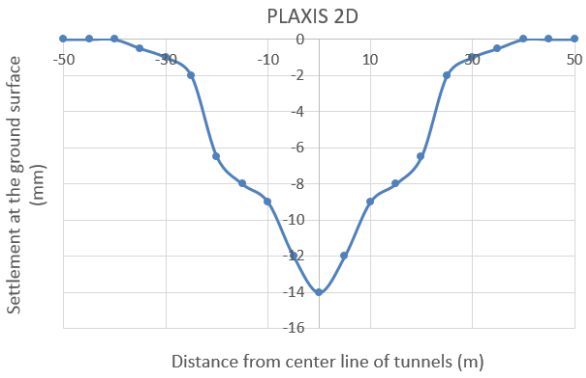

(c)

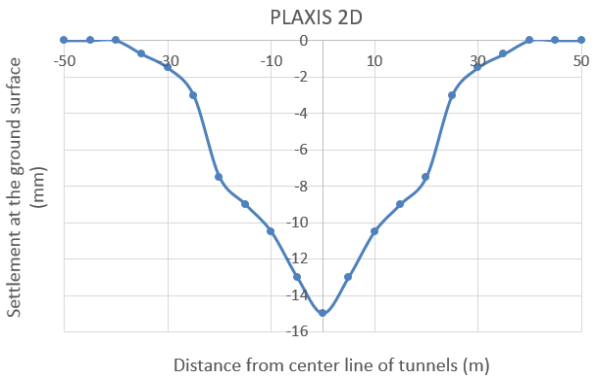

(d)

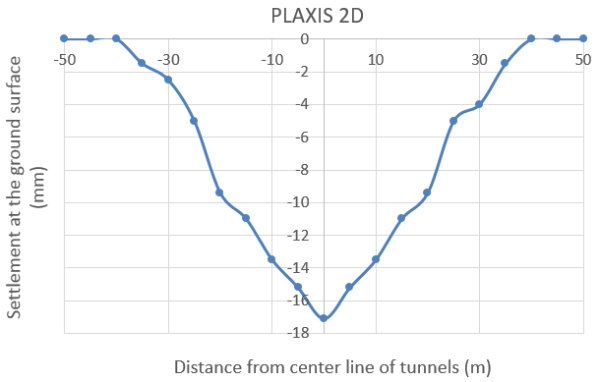

(e)

Fig. 10 Continued

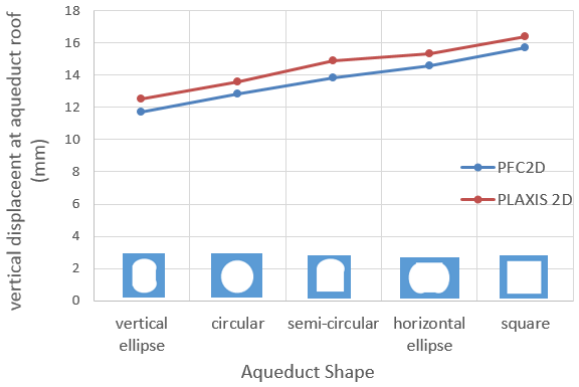

Fig. 11 variation of vertical displacement at Qanat roof based on Qanat shape

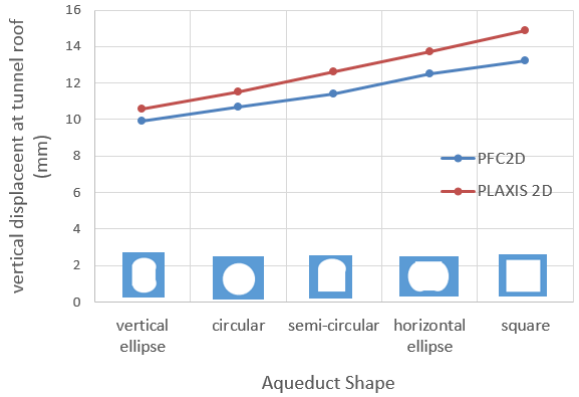

Fig. 12 variation of vertical displacement at tunnel roof based on Qanat shape

force and maximum compressive force in rectangular Qanat, i.e., $5.1*10^5$ N and $2.5*10^4$ N, were more than other cases while they have minimum values in nail Qanat.

4.2 Vertical displacement contour in PLAXIS 2D models

The vertical displacement contour as shown in Figs. 8 a-e illustrates the state of vertical displacement within the modelled samples for five shapes of Qanat (i.e., square, semi-circular, vertical ellipse, circular and horizontal ellipse). The red and blue lines shown in Figs. 16 represent the maximum and minimum displacement in the model, respectively. It can be easily seen that the maximum vertical displacements are concentrated at top and bottom of the spaces. The maximum vertical displacement in the case of rectangular Qanat shape were more than other cases while it has minimum values in vertical ellipse Qanat.

4.3 Settlement of ground surface

Fig. 9 show the settlement of ground surface for five shape of the Qanat at the end of the construction of tunnel and Qanat in PFC2D. DEM results will be compared by the FEM results (Fig 10). It shows that both the settlement pattern and amplitude depend on the Qanat shape. The maximum settlement of ground surface is observed for the square shape of Qanat for both the DEM and FEM (Figs. 9(a) and 10(a)). The minimum settlement of ground surface is observed for the vertical ellipse shape of Qanat for both

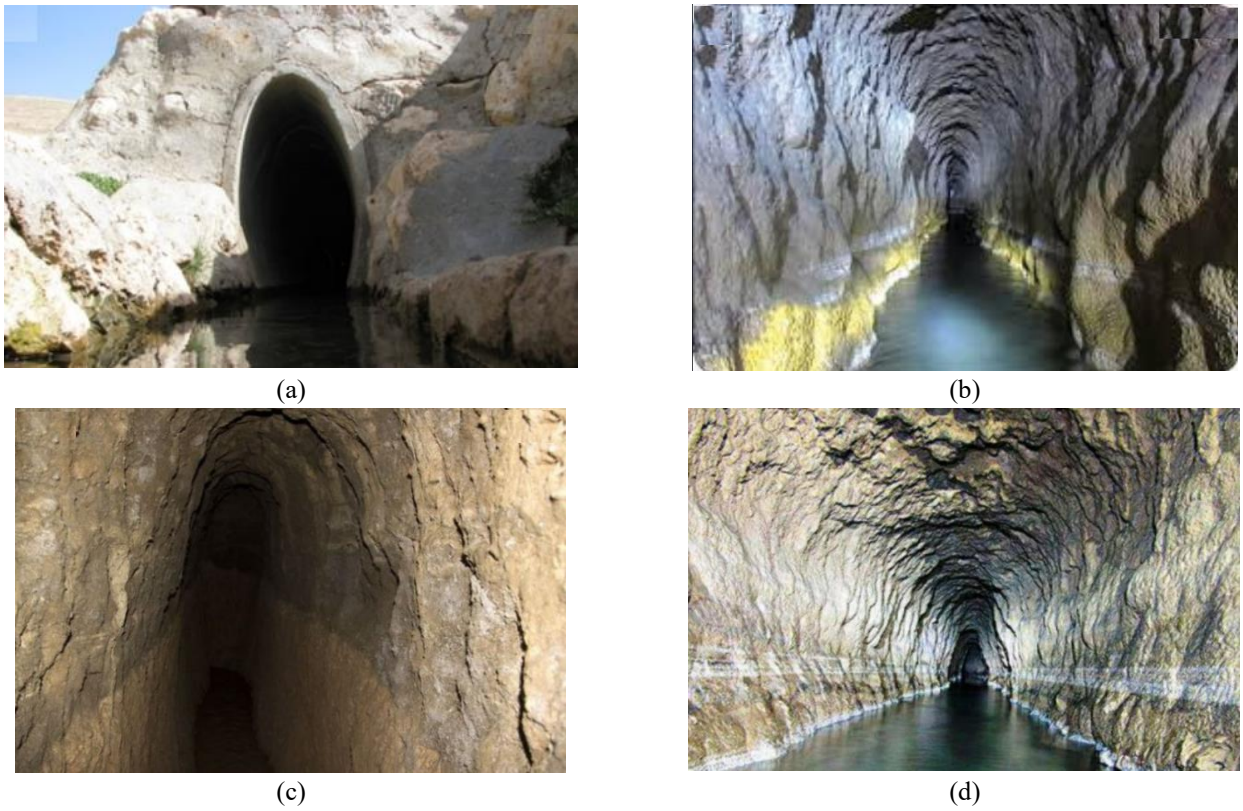

(a) (b)

(c) (d)

Fig. 13 Historical shape of Qanat in Iran

the DEM and FEM (Figs. 9(c) and 10(c)). the results obtained from DEM analysis (Fig. 9) are lower than FEM analysis (Fig. 10) (about 6%). The change in Qanat shape leads to changing of settlement pattern.

4.4. Vertical displacement at Qanat roof

Fig. 11 shows the variation of vertical displacement at Qanat roof based on Qanat shape. The results of PFC2D and PLAXIS2D were depicted in this figure. The minimum vertical displacement at Qanat roof occurred in vertical ellipse shape of Qanat while the maximum vertical displacement occurred in square shape of Qanat. The PLAXIS2D predictions were more than PFC2D simulation outputs. Because the low porosity has been selected for PFC2D simulation.

4.5. Vertical displacement at tunnel roof

Fig 12 shows the variation of vertical displacement at tunnel roof based on Qanat shape. The results of PFC2D and PLAXIS2D were depicted in this figure. The minimum vertical displacement at tunnel roof occurred in vertical ellipse shape of Qanat while the maximum vertical displacement at tunnel roof occurred in square shape of Qanat. The PLAXIS2D predictions were more than PFC2D simulation outputs.

4.6. Historical shape of Qanat

Fig 13 shows the historical shape of Qanat in Iran. This figure shows that the vertical ellipse shape of Qanat has been built in several decade of years ago. This means that the findings of this research is in a good accordance with historical shape of Qanat.

4.7. Restriction

The main concern of DEM modeling is run-times of analyses. For the selected numbers of discs and elements in this paper, the DEM analyses take time approximately 16 times more than FEM analyses (ignoring the time for calibration in DEM). By increasing the numbers of discs and elements, the difference of run-times will be increased.

5. Conclusions

This paper presents analysis of the interaction between tunnel and Qanat with a particular interest for the optimization of Qanat shape using the discrete element code, PFC2D, and the results will be compared with the FEM results of PLAXIS2D. For these concerns, using software PFC2D based on Discrete Element Method (DEM), a model with dimension of 100m * 100 m was prepared. A circular tunnel with dimension of 9 m was situated 20 m below the ground surface. Also one Qanat was situated perpendicularly above the tunnel roof. Distance between Qanat center and ground surface was 8 m. Five different shapes for Qanat were selected i.e., square, semi-circular, vertical ellipse, circular and horizontal ellipse. Confining pressure of 5 MPa was applied to the

model. The vertical displacement of balls situated in ground surface was picked up to measure the ground subsidence. Also two measuring circles were situated at the tunnel roof and Qanat roof to check the vertical displacements.

• Based on the analyses results and Findings, complicated DEM shows advantages and disadvantages with respect to conventional FEM. The main advantages of DEM are modeling the discontinuous nature of soils (more consistent with reality), prevention of surface swelling during unloading in shallow tunnels, more accurate modeling of confining effect with depth and capability of modeling weak bond connections of particles (tensile and shear) in shallow layers. However, the main disadvantages of DEM are higher computational effort and also need for determination of micro-parameters based on calibration.

• The maximum vertical displacements are concentrated at top and bottom of the spaces. The maximum vertical displacement in the case of rectangular Qanat shape were more than other cases while it has minimum values in vertical ellipse Qanat.

• The maximum tensile forces are concentrated at top and bottom of the spaces while the maximum compressive forces are concentrated at left and right sides of the spaces. The both of maximum tensile force and maximum compressive force in rectangular Qanat were more than other cases while they have minimum values in nail Qanat.

• Both the settlement pattern and amplitude depend on the Qanat shape. The maximum settlement of ground surface is observed for the square shape of Qanat for both the DEM and FEM. The minimum settlement of ground surface is observed for the vertical ellipse shape of Qanat for both the DEM and FEM. the results obtained from DEM analysis are lower than FEM analysis (about 6%). The change in Qanat shape leads to changing of settlement pattern.

• The minimum vertical displacement at Qanat roof occurred in vertical ellipse shape of Qanat while the maximum vertical displacement occurred in square shape of Qanat. The PLAXIS2D predictions were more than PFC2D simulation outputs.

• The minimum vertical displacement at tunnel roof occurred in vertical ellipse shape of Qanat while the maximum vertical displacement at tunnel roof occurred in square shape of Qanat. The PLAXIS2D predictions were more than PFC2D simulation outputs.

• The author suggest numerical simulation of Qanat in 3 dimensions.

References

Chan, D., Kodikara, J.K., Gould, S., Ranjith, P.G., Choi, X.S.K., and Davis, P. (2007), "Data analysis and laboratory investigation of the behaviour of pipes buried in reactive clay", *Proceedings of the 10th Australia New Zealand Conference on Geomechanics – Common Ground*, Queensland, Australia, October.

Cundall, P.A. (1971) "A computer model for simulating progressive large scale movements in blocky rock systems", *Proceedings of the Symposium of the International Society of Rock Mechanics*, Nancy, France, September.

Cundall, P.A. and Strack, O.D.L. (1979) "A discrete numerical model for granular assembles", *Geotechnique*, **29**(1), 47-65. https://doi.org/10.1680/geot.1979.29.1.47.

Divall, S. and Goodey, R.J. (2015), "Twin-tunnelling-induced ground movements in clay", *Proc. Inst. Civ. Eng. Geotech. Eng.*, **168**(3), 247-256. https://doi.org/10.1680/geng.14.00054.

Do, N.A., Dias, D., Oreste, P. and Djeran-Maigre, I. (2014), "Three-dimensional numerical simulation of a mechanized twin tunnels in soft ground", *Tunn. Undergr. Sp. Tech.*, **42**, 40-51. https://doi.org/10.1016/j.tust.2014.02.001.

Donze, F.V., Richefeu, V. and Magnier, S.A. (2009), "Advances in discrete element method applied to soil rock and concrete mechanics", *Elec. J. Geol. Eng.*, **8**, 1-44.

Fakhimi, A., Carvalho, T. and Labuz, J.F. (2002), "Simulation of failure around a circular opening in rock", *Int. J. Rock Mech. Min. Sci.*, **39**(4), 507-515. https://doi.org/10.1016/S1365-1609(02)00041-2.

Gould, S., Boulaire, F., Marlow, D. and Kodikara, J. (2009), "Understanding how the Australian climate can affect pipe failure", *Proceedings of OzWater 09 Australia's National Water Conference and Exhibition*, Melbourne, Australia, March.

Greenwood J. (2002) "3D analysis of surface settlement in soft ground tunnelling", Ph.D. Thesis, University of Minnesota, Minneapolis, Minnesota, U.S.A.

Guglielmetti, V., Grasso, P., Mahtab, A. and Xu, S. (2007), *Mechanized Tunnelling in Urban Areas: Design Methodology and Construction Control*, Geodata S.P.A., Turin, Italy, 312-322.

Haeri, H. and Sarfarazi, V. (2016a), "The effect of micro pore on the characteristics of crack tip plastic zone in concrete", *Comput. Concrete*, **17**(1), 107-112. https://doi.org/10.12989/cac.2016.17.1.107.

Haeri, H. and Sarfarazi, V. (2016b), "The effect of non-persistent joints on sliding direction of rock slopes", *Comput. Concrete*, **17**(6), 723-737. https://doi.org/10.12989/cac.2016.17.6.723.

Haeri, H. and Sarfarazi, V. (2016c), "The deformable multilaminate for predicting the elasto-plastic behavior of rocks", *Comput. Concrete*, **18**(2), 201-214. https://doi.org/10.12989/cac.2016.18.2.201.

Haeri, H., Sarfarazi, V. and Lazemi, H.A. (2016d), "Experimental study of shear behavior of planar non-persistent joint", *Comput. Concrete*, **17**(5), 639-653. https://doi.org/10.12989/cac.2016.17.5.639.

Hage Chehade F. and Shahrour I. (2008), "Numerical analysis of the interaction between twin-tunnels: Influence of the relative position and construction procedure", *Tunn. Undergr. Sp. Tech.*, **23**(2), 210-214. https://doi.org/10.1016/j.tust.2007.03.004.

Harris, D.I., Mair, R.J., Love, JP., Taylor, R.N. and Henderson, T.O. (1994), "Observations of ground and structure movements for compensation grouting during tunnel construction at Waterloo station", *Geotechnique*, **44**(4), 691-713. https://doi.org/10.1680/geot.1994.44.4.691.

Hu, J., Wen, G., Lin, Q., Cao, P. and Li, S. (2020), "Mechanical properties and crack evolution of double-layer composite rock-like specimens with two parallel fissures under uniaxial compression", *Theor. Appl. Fract. Mech.*, **108**, 102610. https://doi.org/10.1016/j.tafmec.2020.102610.

Itasca Consulting Group, Inc. (2004), PFC2D, Particle Flow Code in 2 Dimensions, Version 3.

Jiang, M. and Yin, Z.Y. (2012), "Analysis of stress redistribution in soil and earth pressure on tunnel lining using the discrete element method", *Tunn. Undergr. Sp. Tech.*, **32**, 251-259. https://doi.org/10.1016/j.tust.2012.06.001.

Jiang, M. and Yin, Z.Y. (2014), "Influence of soil conditioning on ground deformation during longitudinal tunneling", *Comptes Rendus Mécanique*, **342**(3), 189-197. https://doi.org/10.1016/j.crme.2014.02.002.

Jin, Y.F., Yin, Z.Y., Zhou, W.H. and Huang, H.W. (2019), "Multi-objective optimization-based updating of predictions during excavation", *Eng. Appl. Artif. Intel.*, **78**, 102-123. https://doi.org/10.1016/j.engappai.2018.11.002.

Kanou, S., Amano, M., Terasaka, Y., Matsumoto, N. and Wada, T. (2003), "Terra-mechanical simulation using distinct element method", KOMAT'SO Technical Report, 13-14.

Katebi, H., Rezaei, A.H., Hajialilue-Bonab, M. and Tarifard, A. (2015), "Assessment the influence of ground stratification, tunnel and surface buildings specifications on shield tunnel lining loads (by FEM)", *Tunn. Undergr. Sp. Tech.*, **49**, 67-78. https://doi.org/10.1016/j.tust.2015.04.004.

Li, P., Du, S.J., Ma, X.F., Yin, Z.Y. and Shen, S.L. (2014), "Centrifuge investigation into the effect of new shield tunnelling on an existing underlying large-diameter tunnel", *Tunn. Undergr. Sp. Tech.*, **42**, 59-66. https://doi.org/10.1016/j.tust.2014.02.004.

Liao, S.M., Peng, F.L. and Shen, S.L. (2008), "Analysis of shearing effect on tunnel induced by load transfer along longitudinal direction", *Tunn. Undergr. Sp. Tech.*, **23**(4), 421-430. https://doi.org/10.1016/j.tust.2007.07.001.

Lin, Q., Cao, P., Cao, R., Lin, H. and Meng, J. (2020a), "Mechanical behavior around double circular openings in a jointed rock mass under uniaxial compression", *Arch. Civ. Mech. Eng.*, **20**(1), 1-18. https://doi.org/10.1007/s43452-020-00027-z.

Lin, Q., Cao, P., Meng, J., Cao, R. and Zhao, Z. (2020b), "Strength and failure characteristics of jointed rock mass with double circular holes under uniaxial compression: Insights from discrete element method modelling", *Theor. Appl. Fract. Mech.*, **109**, 102692. https://doi.org/10.1016/j.tafmec.2020.102692.

Liu, H., Li, P. and Liu, J. (2011), "Numerical investigation of underlying tunnel heave during a new tunnel construction", *Tunn. Undergr. Sp. Tech.*, **26**(2), 276-283. https://doi.org/10.1016/j.tust.2010.10.002.

Moller, S.C. (2006), *Tunnel Induced Settlements and Structural Forces in Linings*, in *Geotechnik*, University of Stuttgart, Inst. f., Stuttgart, Germany, 108-125.

Ng, C.W.W., Liu, G.B. and Li, Q. (2013), "Investigation of the long-term tunnel settlement mechanisms of the first metro line in Shanghai", *Can. Geotech. J.*, **50**(6), 674-684. https://doi.org/10.1139/cgj-2012-0298.

Pratt, C., Yang, H., Hodkiewicz, M. and Oldham, S. (2011), "Factors influencing pipe failures in the WA environment", *Proceedings of the Co-operative Education for Enterprise Development CEED Seminar*, Perth, Australia.

Sarfarazi, V. and Haeri, H. (2016a), "Effect of number and configuration of bridges on shear properties of sliding surface", *J. Min. Sci.*, **52**(2), 245-257. https://doi.org/10.1134/S1062739116020370.

Sarfarazi, V., Faridi, H.R., Haeri, H. and Schubert, W. (2016b), "A new approach for measurement of anisotropic tensile strength of concrete", *Adv. Concrete Construct.*, **3**(4), 269-284. http://doi.org/10.12989/acc.2015.3.4.26

Sarfarazi, V., Ghazvinian, A., Schubert, W., Blumel, M. and Nejati, H.R. (2014), "Numerical simulation of the process of fracture of Echelon rock joints", *Rock Mech. Rock Eng.*, **47**(4), 1355-1371. http://doi.org/10.1007/s00603-013-0450-3.

Sarfarazi, V., Haeri, H. and Khaloo, A. (2016c), "The effect of non-persistent joints on sliding direction of rock slopes", *Comput. Concrete*, **17**(6), 723-737. https://doi.org/10.12989/cac.2016.17.6.723.

Shen, S.L. and Xu, Y.S. (2011), "Numerical evaluation of land subsidence induced by groundwater pumping in Shanghai", *Can. Geotech. J.*, **48**(9), 1378-1392. https://doi.org/10.1139/t11-049.

Tan, Y. and Wei, B. (2011), "Observed behaviors of a long and deep excavation constructed by cut-and-cover technique in Shanghai soft clay", *J. Geotech. Geoenviron. Eng.*, **138**(1), 69-88. https://doi.org/10.1061/(ASCE)GT.1943-5606.0000553.

Tian, X. (2020), "A theoretical calculation method of influence radius of settlement based on the slices method in tunnel construction", *Math. Prob. Eng.*, **4**, 212-230. https://doi.org/10.1155/2020/5804823.

Wang J.G., Kong S.L and Leung C.F. (2003) "Twin tunnel induced ground settlement in soft soils", *Proceedings of the SINO-JAPANESE Symposium on Geotechnical Engineering*, Beijing, China, October.

Yang, X.L. and Wang, J.M. (2011), "Ground movement prediction for tunnels using simplified procedure", *Tunn. Undergr. Sp. Tech.*, **26**(3), 462-471. https://doi.org/10.1016/j.tust.2011.01.002.

Zhang, Z.X., Liu, C., Huang, X., Kwok, C.Y. and Teng, L. (2016), "Three-dimensional finite-element analysis on ground responses during twin-tunnel construction using the URUP method", *Tunn. Undergr. Sp. Tech.*, **58**, 133-146. https://doi.org/10.1016/j.tust.2016.05.001.

Zhang, Z. and Huang, M. (2014), "Geotechnical influence on existing subway tunnels induced by multiline tunneling in Shanghai soft soil", *Comput. Geotech.*, **56**, 121-132. https://doi.org/10.1016/j.compgeo.2013.11.008.

Zhang, Z., Huang, M., Zhang, C., Jiang, K. and Lu, M. (2019), "Time domain analyses for pile deformation induced by adjacent excavation considering influences of viscoelastic mechanism", *Tunn. Undergr. Sp. Tech.*, **85**(3), 392-405. https://doi.org/10.1016/j.tust.2018.12.020.

Zhang, Z., Huang, M. and Wang, W. (2013), "Evaluation of deformation response for adjacent tunnels due to soil unloading in excavation engineering", *Tunn. Undergr. Sp. Tech.*, **38**(9), 244-253. https://doi.org/10.1016/j.tust.2013.07.002.

Zhang, Z., Pan, Y., Zhang, M., Lv, X., Jiang, K. and Li, S. (2020), "Complex variable analytical prediction for ground deformation and lining responses due to shield tunneling considering groundwater level variation in clays", *Comput. Geotech.*, **120**(4), 103443. https://doi.org/10.1016/j.compgeo.2020.103443.

Zhang, Z., Huang, M., Zhang, C., Jiang, K., Wang, Z. and Xi, X. (2020), "Complex variable solution for twin tunneling-induced ground movements considering non-uniform convergence pattern", *Int. J. Geomech.*, **20**(6), 04020060. https://doi.org/10.1061/(ASCE)GM.1943-5622.0001700.

Zhang, Z., Huang, M., Zhang, C., Jiang, K. and Bai, Q. (2020), "Analytical prediction of tunneling-induced ground movements and liner deformation in saturated soils considering influences of shield air pressure", *Appl. Math. Model.*, **78**, 749-772. https://doi.org/10.1016/j.apm.2019.10.025.

Zhang, Z., Huang, M., Zhang, C., Jiang, K. and Lu, M. (2019), "Time-domain analyses for pile deformation induced by adjacent excavation considering influences of viscoelastic mechanism", *Tunn. Undergr. Sp. Tech.*, **85**(3), 392-405. https://doi.org/10.1016/j.tust.2018.12.020.

Zhang, Z., Huang, M., Xu, C., Jiang, Y. and Wang, W. (2018), "Simplified solution for tunnel-soil-pile interaction in Pasternak's foundation model", *Tunn. Undergr. Sp. Tech.*, **78**(8), 146-158. https://doi.org/10.1016/j.tust.2018.04.025.

Zhang, Z., Huang, M., Xi, X. and Yang, X. (2018), "Complex variable solutions for soil and liner deformation due to tunneling in clays", *Int. J. Geomech.*, **18**(7), 04018074. https://doi.org/10.1061/(ASCE)GM.1943-5622.0001197.

IC